Separation Science and Technology
Publication details, including instructions for authors and subscription information:
http://www.informaworld.com/smpp/title~content=t713708471

Synthesis of Silica Nanofluid and Application to CO_2 Absorption

Wun-gwi Kim[a]; Hyun Uk Kang[a]; Kang-min Jung[a]; Sung Hyun Kim[a]
[a] Department of Chemical and Biological Eng., Korea University,

Online publication date: 22 June 2010

To cite this Article Kim, Wun-gwi , Kang, Hyun Uk , Jung, Kang-min and Kim, Sung Hyun(2008) 'Synthesis of Silica Nanofluid and Application to CO_2 Absorption', Separation Science and Technology, 43: 11, 3036 — 3055
To link to this Article: DOI: 10.1080/01496390802063804
URL: http://dx.doi.org/10.1080/01496390802063804

Separation Science and Technology, 43: 3036–3055, 2008

ISSN: 0149-6395 print/1520-5754 online
DOI: 10.1080/01496390802063804

Taylor & Francis
Taylor & Francis Group

Synthesis of Silica Nanofluid and Application to CO_2 Absorption

Wun-gwi Kim, Hyun Uk Kang, Kang-min Jung, Sung Hyun Kim
Department of Chemical and Biological Eng., Korea University

Abstract: This study focused on the synthesis of stable nanofluids and their direct application to the CO_2 absorption process. A sol-gel process was used as the synthesis method of nanoparticles in nanofluid. The particle size and stability were determined by SEM image and zeta potential of the nanofluid. Three types of nanofluids containing approximately 30 nm, 70 nm, and 120 nm particles were synthesized and all nanofluids had a stable zeta potential of approximately −45 mV. Addition of nanoparticles increased the average absorption rate of 76% during the first 1 minute and total absorption amount of 24% in water. The capacity coefficient of CO_2 absorption in the nanofluid is 4 times higher than water without nanoparticles, because the small bubble sizes in the nanofluid have large mass transfer areas and high solubility.

Keywords: Absorption, CO_2, mass transfer, nanofluid, nanoparticle

INTRODUCTION

A nanofluid is a stable suspension containing nanoparticles. The nanofluid can be prepared by common methods for synthesizing nanoparticles. Many researchers are developing novel methods for the synthesis of nanoparticles. Xun et al. (1) prepared the stable silver nanoparticles using the extraction reduction method. Christopher et al. (2) synthesized the copper nanoparticles in compressed liquid and supercritical fluid reverse micelle systems. Lai et al. (3) controlled the size of the magnetic nanoparticles using a blockcopolymer.

Received 19 June 2007; accepted 21 January 2008.
Address correspondence to Sung Hyun Kim, Department of Chemical and Biological Eng., Korea University. E-mail: kimsh@korea.ac.kr

Since the term "nanofluid" for enhancing heat transfer was firstly used by Choi (4), there have been considerable efforts in investigating nanofluids with practical application to heat transfer. Many researchers have reported the high thermal conductivity and heat transfer coefficient of nanofluids (5,6). Keblinski et al. (7) suggested the possible mechanisms for the heat transfer of nanofluids as the brownian motion of nanoparticles, liquid layering, particle clustering, and the thermal properties of the medium. Krishnamurthy et al. (8) first observed that a dye diffuses faster in a nanofluid than in water. They explained that the Brownian motion of the nanoparticles induces convection in the nanofluids. Ha (9) reported that the absorption rate of ammonia in water was increased by the addition of nanoparticles in a falling film type absorber. Kim et al. (10) reported the increased ammonia absorption performance by the addition of nanoparticles in a bubble type absorber.

One of the most important absorption application used by nanofluids is the CO_2 absorption. The reduction of CO_2 is becoming more important in these days. In terms of the Kyoto Protocol, many nations have set targets for decreasing the CO_2 gas emissions. Several studies have proposed various methods to enhance the CO_2 absorption efficiency. Astarita (11) used a Mono Ethanol Amine (MEA) solution to enhance the absorption performance by a reaction between the MEA and CO_2. However, this method has some flaws such as the corrosion of the reactors by the amine component and the difficulty in renewable operation. Therefore, Chakraborty et al. (12) used the hindered amine and made an effective regeneration of a concentrated absorbent. An increased resistance to the SO_2 component is a weak point of the hindered amine process. Rao (13) reported the Hot Potassium Carbonate (HPC) process. Cullinane and Derks (14,15) used a piperazine material to enhance the level of CO_2 absorption and effective regeneration processes. As a physical approach for enhancing CO_2 absorption, Dagaonkar et al. (16) developed an adsorption method by attaching the gas components to TiO_2 microparticles.

Although these methods for enhancing the absorption performance are useful, these are highly dependent on the specific properties of the target material, such as the surface structure of microparticles and the reaction kinetics of each component. Because of these reasons, a nanofluid is suggested as a new absorbent to increase the rate of CO_2 absorption. Kim et al. (17) reported that gas bubbles in a nanofluid are smaller than in pure water and applied this phenomenon directly to a gas absorption process in a bubble type absorber.

The aims of this study are to synthesize the stable nanofluids and determine their CO_2 absorption performance. The solution containing K_2CO_3 and piperazine was also used as the absorbent, and the combined performances with the nanofluids were investigated.

THEORY

Sol-gel Method

In this research, silica nanofluids were used, because it is the widely used material and easy to prepare. The electric insulating properties of silica nanoparticles also suggest potential applications to electronic devices.

The sol-gel method is a widely used process for synthesizing nanoparticles. Figure 1 shows the reaction mechanisms of the sol-gel process for the synthesis of silica nanoparticles. The reaction passes by two steps. The first step is the hydrolysis reaction of the precursors and the next step is the condensation. In the hydrolysis reaction, the organic binders of the precursors are substituted with hydroxyl groups and two hydrolyzed monomers are connected to each other in the condensation step. For synthesis of spherical particles, the processes are performed under base condition (18). Because the rate of the hydrolysis reaction is much faster than the condensation process in the base catalysis. The condensation reaction occurs after all the organic binders of the precursors are substituted with hydroxyl groups. They can be grown to spherical particles with a network structure. The reaction rate at each step is determined by pH, temperature and concentration of each component. The particle sizes and shapes can be regulated by changing these independent variables.

DLVO Theory

Interparticle forces should be considered for analyzing stability of nanoparticles in a synthesized nanofluid. The DLVO theory was named after

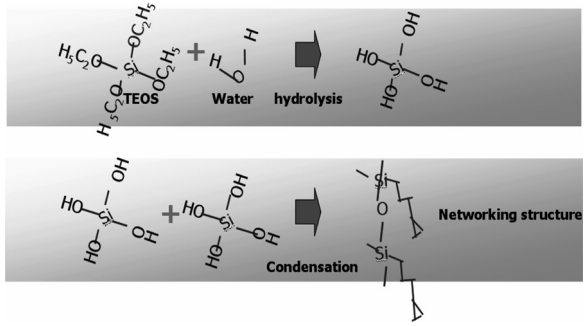

Figure 1. Reaction mechanism of the sol-gel process for the synthesis of silica nanoparticles.

Derjaguin, Landau, Verwey, and Overbeek(DLVO) and provided the basic framework for the colloidal interactions and stability (19). There are interaction forces of two types. One is the van der Waals attractive force between particles. The other one is the repulsive force acquired as a result of the surface charge or specific ion adsorption. Equations (1) $\sim$(3) give the mathematical descriptions for the interparticle forces. At the equilibrium point of the two forces, when the total potential energy is zero, the particles will be arranged at a stable distance.

$$\text{Van der waals attractive Energy} : V_A = -\frac{A}{12\pi} d^{-2} \tag{1}$$

$$\text{Double layer repulsive Energy} : V_R = V_0 \exp(-kd) \tag{2}$$

$$\text{Total potential Energy} : V_T = V_A + V_R \tag{3}$$

Zeta potential is a widely used factor for quantifying particle stability. Zeta potential means the surface charge at the stern (slipping) layer of the particles. The ionic group of particles attract the opposite ions and establish the ion cloud, which determines the zeta potential value. If the absolute value of zeta potential were too low, the particles would aggregate. On the other hand, if the absolute value of the zeta potential is high, the particles would be separated by a stable condition.

Fig. 2 shows the various ways to induce a repulsive force and make the particles stable. The representative nature of the double layer repulsive force is the steric and electrostatic hindrance. With this principle, the particles will be stable by inducing a surface charge and attaching polymer chains to the particle surface. The high concentration of ions and polymer chains between the two particles attached by surface treatment induces an osmotic pressure and makes the particles separate.

Reaction Kinetics

In this study, piperazine promoted potassium carbonate was used as the reacting absorbent to the CO_2 gas. Potassium ions in potassium carbonate store aqueous CO_2 in solution. Piperazine is the organic compound that has a six-membered ring with two opposing amine functional groups. Table 1 shows the structure of piperazine and the individual reactions when CO_2 absorption occurs in this solution. Like the reaction kinetics, piperazine is an attractive material for absorbing CO_2, because two CO_2 molecules can be attached to a single piperazine molecule through the two amine functional groups in piperazine.

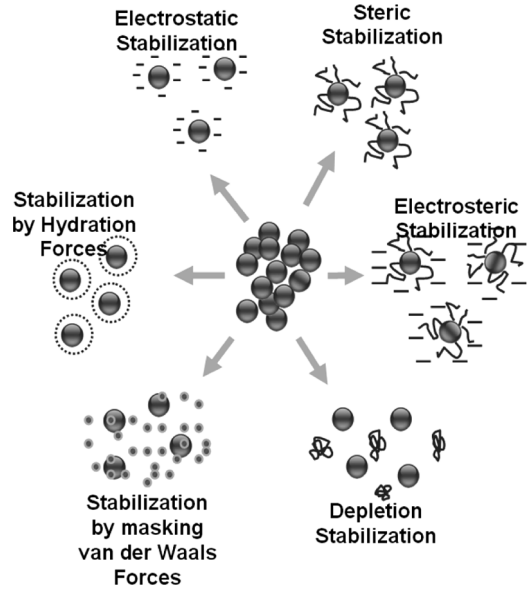

Figure 2. Various methods for inducing particle stability.

In addition, the CO_2 is detached easily due to the steric hindrance in the piperazine molecule. This can be quite beneficial to the process of regeneration of the concentrated absorbent.

Table 1. Reaction kinetics of CO_2 in the PZ promoted potassium carbonate solution

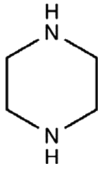 Structure of piperazine
$CO_2(g) \leftrightarrow CO_2(aq)$
$CO_2(aq) + 2H_2O \leftrightarrow HCO_3^- + H_3O^+$
$HCO_3^- + H_2O \leftrightarrow CO_3^{2-} + H_3O^+$
$2H_2O \leftrightarrow H_3O^+ + OH^-$
$PZ + H_2O + CO_2(aq) \leftrightarrow PZCOO^- + H_3O^+$
$PZH^+ + H_2O \leftrightarrow PZ + H_3O^+$
$PZCOO^- + H_2O + CO_2(aq) \leftrightarrow PZ(COO^-)_2 + H_3O^+$
$H^+PZCOO^- + H_2O \leftrightarrow PZ(COO^-) + H_3O^+$

EXPERIMENTAL

Preparation of Nanofluid

Rao et al. (20) introduced a simple method for synthesizing silica nanoparticles. The sol-gel process of one step method was used to prepare silica nanofluid. The raw materials for synthesis were TEOS (Tetra Ethyl Ortho Silicate, Aldrich) as the precursor, ethanol (99%, Aldrich) as the solvent, water (DI water) for the hydrolysis reaction, and ammonium hydroxide (NH_3 28%, Aldrich) as the base catalyst. All synthetic processes were performed in an ultra-sonication bath, which made the particle size uniform and induced a stable condition of the homogeneous reaction.

Ethanol of 8 mol and water of 14 mol were placed in a synthesis reactor and stirred for 10 minutes to make the reaction condition homogeneous. Subsequently, TEOS of 0.045 mol was added to the solution and the hydrolysis reaction proceeded. After 20 minutes, ammonium hydroxide was added to promote the condensation process. The synthesis takes approximately 60 minutes after adding the ammonium hydroxide catalyst. The nanoparticles size was regulated by changing the amount of ammonium hydroxide as 0.28 mol, 0.42 mol and 0.56 mol.

Characterization of the Nanofluid

The samples for detecting sizes and shapes of the synthesized nanoparticles were prepared by spin coating the nanofluid onto a silicon oxide wafer. Scanning electron microscopy (SEM) was used to observe and measure the size of the nanoparticles in nanofluid. A zeta-potential meter (ELS-8000, Otsuka Electronics Co.) was used to measure the zeta potential and determine the stability of the produced nanofluid.

Apparatus

Absorption experiments were performed in the bubble type absorber shown in Fig. 3. The absorber was a cylinder of 260 mm (L) $\times$ 70 mm (D) in size. The CO_2 bubbles are injected through the bubbler at the lower part. A mass flow controller (MFC) and mass flow meter (MFM) were used to measure the input and output gas flow rate. The rate of absorption was obtained by subtracting the output gas from the input gas flow rate under airtight conditions. Because the bubble type absorber is a batch reactor, unsteady-state absorption will be performed until the absorbent is saturated. During the experiments,

Figure 3. Schematic diagram of a bubble type absorber.

the gas flow rate the and amount of absorbent were fixed to 0.5 L/min and 0.5 L, respectively, and the absorption experiments were performed at room temperature and 1 atm.

RESULTS AND DISCUSSION

Characterization of Nanoparticles in Nanofluid

Figure 4 shows SEM images of the uniform sized nanoparticles in the nanofluids. The size of the nanoparticles was controlled by the amount of ammonium hydroxide as a catalyst. The particle size was approximately 30 nm, 70 nm, and 120 nm at ammonium hydroxide concentrations of 0.28 mol, 0.42 mol, and 0.56 mol, respectively. The catalyst promotes the condensation reaction in the sol-gel process and the particles grow fast and become large. The number of nanoparticles is small at a large amount of ammonium hydroxide, because the precursor content was fixed in three samples.

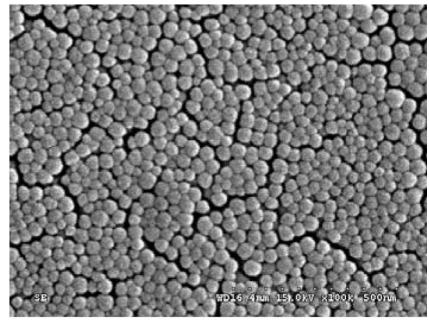

(a) 30 nm (NH_4OH 0.28 mol)

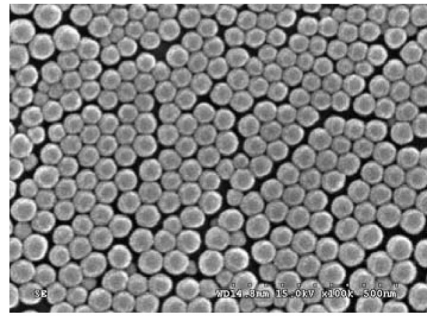

(b) 70 nm (NH_4OH 0.42 mol)

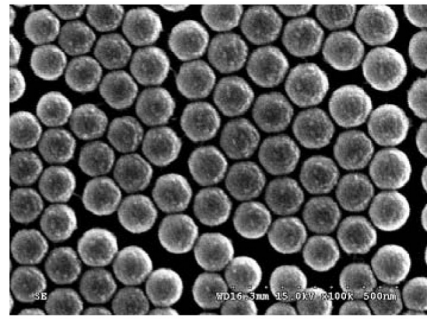

(c) 120 nm (NH_4OH 0.56 mol)

Figure 4. The SEM images of the synthesized nanoparticles in a nanofluid.

The content of the precursors was relatively small compared with the other raw materials under the assumed conditions almost all precursors had changed to silica particles. The synthesis reaction was regarded as the

100% irreversible reaction and expected to produce the same silica particles of 0.045 mol as the amount of precursor. The weight fraction of silica was calculated by the weight of produced silica over the total weight of solution. The calculated weight fraction of nanoparticles in the synthesized nanofluid was approximately 0.42 wt%. The absorption experiment was carried out at nanofluid solution of 0.021 wt% diluted by 20 times.

STABILITY OF THE NANOFLUID PRODUCED

Figure 5 shows the zeta-potential value of the three types of synthesized nanofluid. The absolute values of -44.51 mV, -45.64 mV, and -44.09 mV, were relatively high, which demonstrates the stable nanofluids. Figure 6 shows the electron penetration flows of the cells in the zeta potential experiment and a parabolic curve. The principle of the zeta potential is an electrophoresis method. The electron penetration flows of the solvent due to the surface charge of the cell are involved in determining the zeta potential. Hence, the zeta potential should be measured at the isoelectric point in the electron penetration graph. Both an accurate isoelectric point and zeta potential can be obtained from this parabolic curve of the electron penetration flows.

Gas Absorption in Bubble Type Absorber

Absorption Performance of CO_2

Figure 7 shows images of the bubbles in the water and the nanofluid of 0.021 wt% silica containing 30 nm silica nanoparticles. The bubble size in the nanofluid was much smaller than in the water. This suggests applications to the gas absorption processes such as removing the harmful gases of factory stacks with its large surface area.

Figure 8 shows the absorption rate of CO_2 in water and in the nanofluid as a function of time. The nanofluid contains 0.021 wt% of 30 nm silica nanoparticles. The absorption rate was decreased by the time due to the absorber of a batch reactor. In graph (a), the average rate of absorption during the first 1 minute was 0.253 L/min in water and 0.442 L/min in the nanofluid; the absorption rate was increased 76% in nanofluid. The cumulative absorption curve (b) shows that the overall absorption in the nanofluid was increased 24%.

A piperazine and potassium carbonate solution is an attractive absorbent for the CO_2 absorption. In Fig. 9, the absorption performance in the K_2CO_3 and piperazine solution increased in comparison to water. For the preparation of this absorbent, 0.025 mol of K_2CO_3 and 0.025 mol

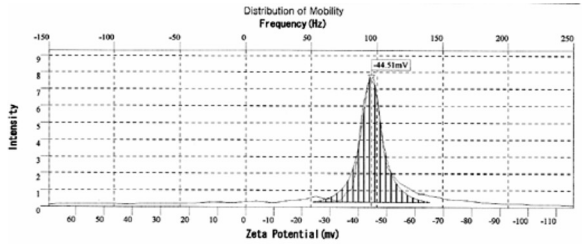

(a) -44.51mV (30 nm)

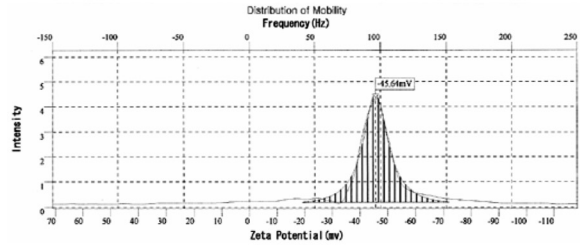

(b) -45.64mV (70 nm)

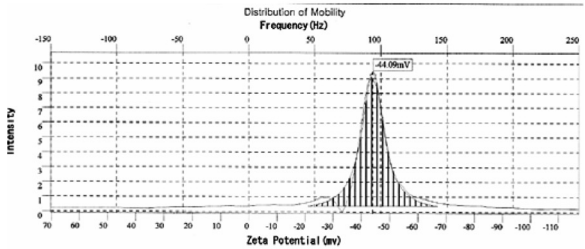

(c) -44.09mV (120 nm)

Figure 5. The zeta potential of the synthesized nanofluids.

of piperazine were dissolved in 1 L of pure water. Figure 9 shows the nanoparticle effects on the absorption rate and amount in the K_2CO_3 and piperazine solution. The average rate of CO_2 absorption during the first 1 minute in the K_2CO_3/piperazine solution, and the K_2CO_3/piperazine solution containing the 0.021 wt% silica nanoparticles were 0.438 L/min and 0.484 L/min respectively, showing an 11% increase. The total absorption in each absorbent was 1.02 L and 1.14 L respectively, indicating a 12% increase.

For the in-depth study on the absorption performance, the mass balance equation for gas absorption in the bubble type absorber was

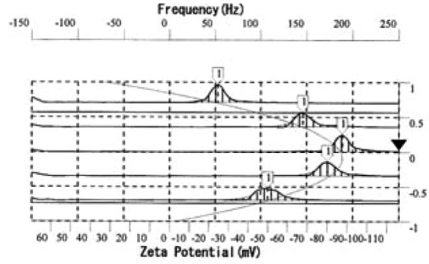

(a) 30nm nanofluid

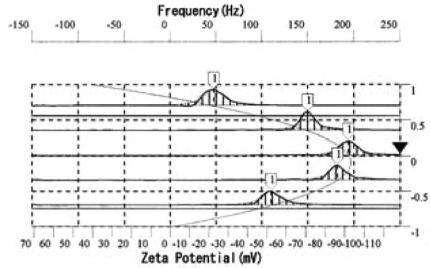

(b) 70 nm nanofluid

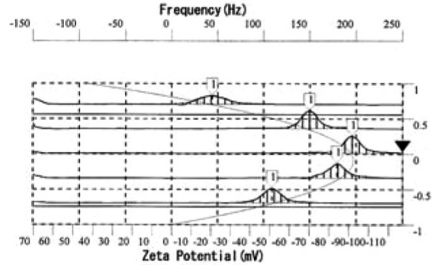

(c) 120 nm nanofluid

Figure 6. Electron penetration flow of the synthesized nanofluids in the zeta potential experiment.

established in equation (4), and this ordinary differential equation can be transformed to equation (5) in case of no reaction (21).

$$w_A = V\frac{dC_A}{dt} = Vk_La(C_{A,s} - C_A) - VR_A \tag{4}$$

$$C_A = C_{A,s}\left[1 - \frac{1}{e^{k_L at}}\right] \tag{5}$$

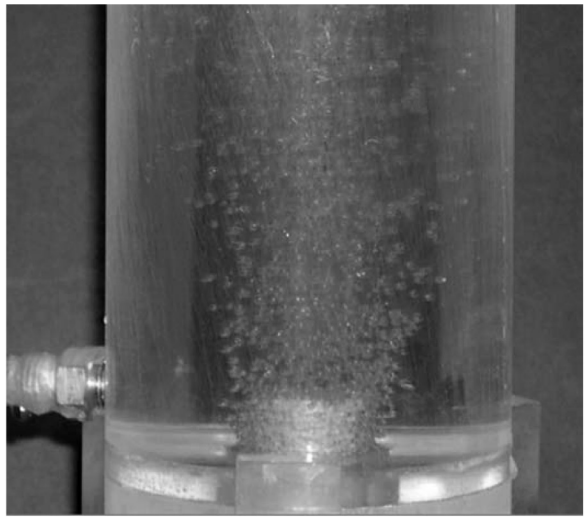

(a) In water

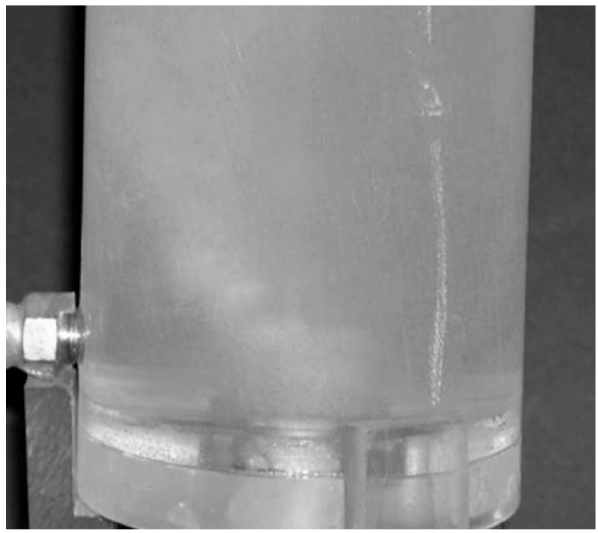

(b) In 0.021 wt% nanofluid

Figure 7. Bubble sizes in water and the nanofluid.

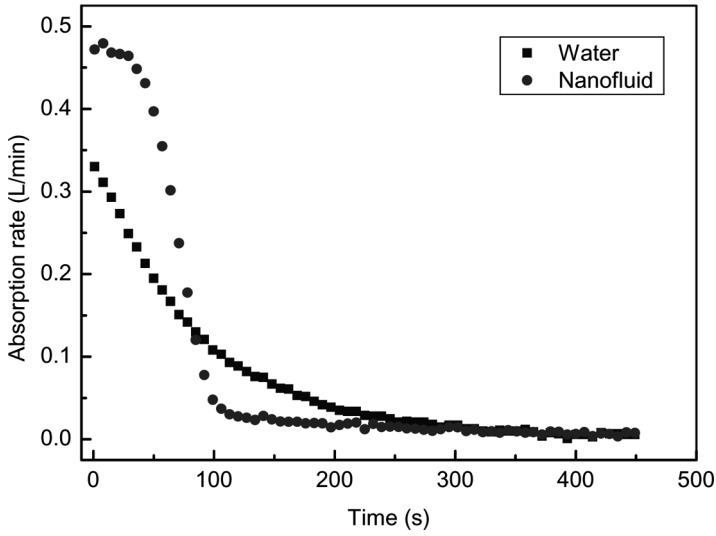

(a)

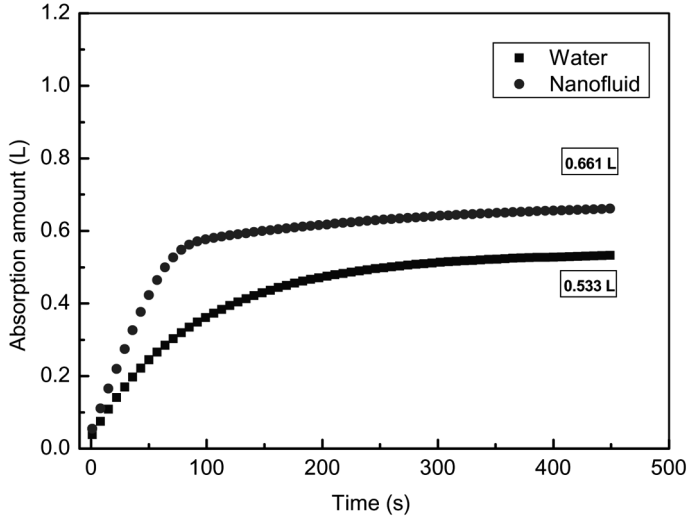

(b)

Figure 8. Absorption rate and absorption amount in water and the nanofluid.

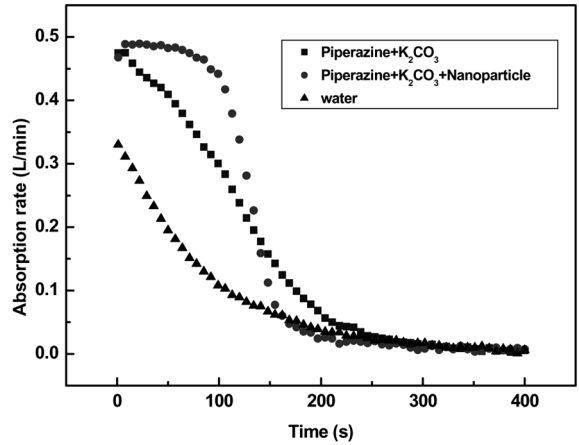

(a)

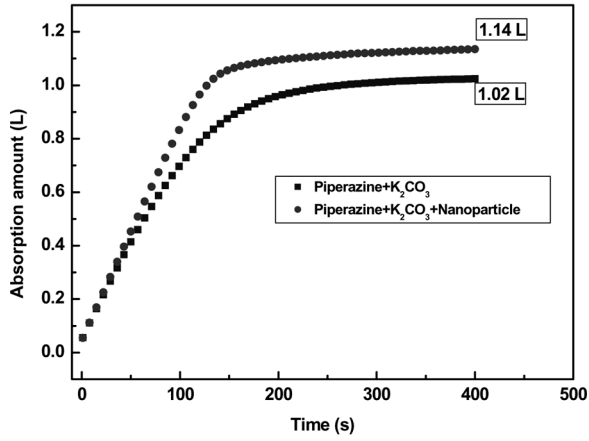

(b)

Figure 9. Absorption rate and amount in the Piperazine/Pottasium Carbonate solution and in the Piperazine/Pottasium Carbonate solution containing 0.021 wt% nanoparticles.

In Fig. 10, the capacity coefficient was obtained by plotting the experimental data along side the derived equation. As a result, the capacity coefficients of the nanofluid and water were 0.045 s^{-1} and 0.0105 s^{-1}, respectively, which show a 329% increase in the nanofluid compared with pure water. The initial flat region in the graph of the nanofluid was attributed to the surface renewal effect induced by collisions between the nanoparticle and flowing bubbles (17).

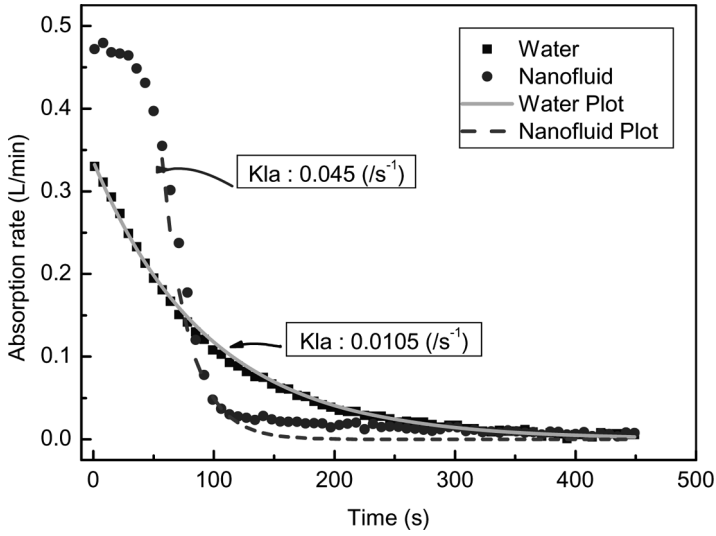

Figure 10. Capacity coefficient in water and the nanofluid.

There is one point that needs to be considered. Even though the experimental data of water was fitted precisely to the derived exponential equation, the experimental data of the nanofluid was not fitted to the exponential equation from approximately 120 s to 400 s. This is explained by the adsorption effect of CO_2 on the surface of the nanoparticles (11). The CO_2 micro bubbles adsorbs onto the surface of the nanoparticles and

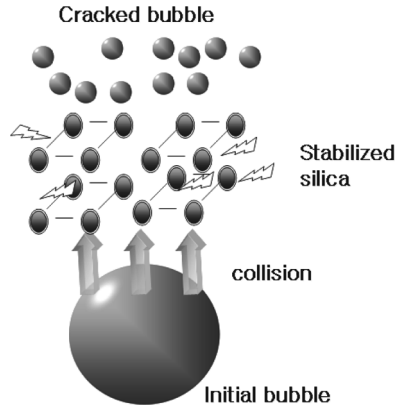

Figure 11. Absorption mechanisms in the bubble type absorber.

the adsorbed gas bubbles increases the absorption performance with the absorption to the solution.

The difference between the equation and experimental value is the additional effects by the adsorption of CO_2 bubbles onto the surface of the nanoparticles. An increasing amount could be obtained by integrating the unmatched region in the graph. The additional effect was determined to be approximately 0.0921 L.Kim et al. (17) suggested possible mechanisms for the CO_2 absorption in a nanofluid. The absorption mechanism is illustrated in Fig. 11. The stable nanoparticles in a nanofluid provide additional energy to the solution and increase the total area of gas bubbles. This means that the stable nanoparticles and flowing gas bubbles collide with each other and gas bubbles are cracked to small bubbles and the mass transfer area is increased. This phenomenon was optically observed in the absorber in Fig. 7.

This small bubble size enlarges the total absorption amount and increases the inner bubble pressure by the Laplace-Young equation (6). In addition, from Kelvin equation (7), the solubility of the gas component increases when the radius of the gas bubbles decreases (22). This principle can explain the increases in the total absorption amount in the experimental results of the nanofluid.

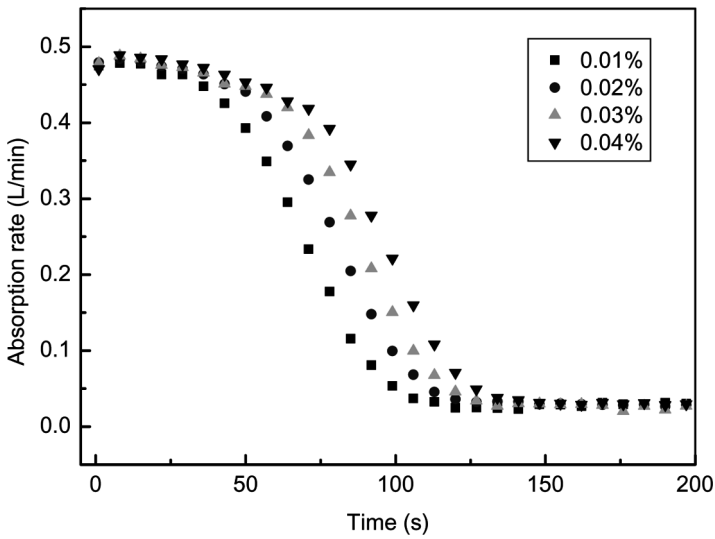

Figure 12. Nanoparticle concentration effects on the absorption performance in nanofluid.

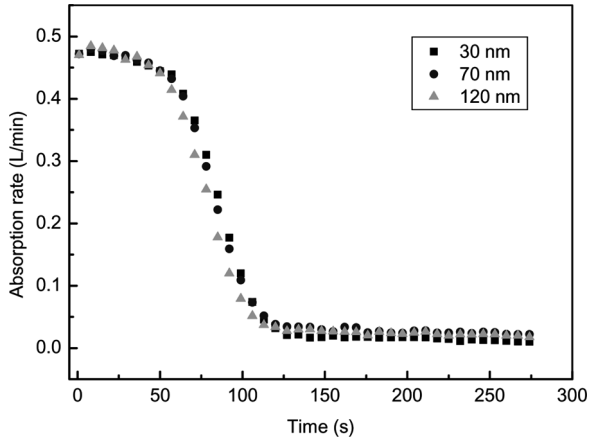

Figure 13. Nanoparticle size effect on absorption performance in the nanofluid.

Laplace Young equation:

$$\Delta p = p_{in} - p_{out} = \frac{2\gamma}{R} \tag{6}$$

Kelvin equation:

$$RT \ln \frac{P}{P_0} = \frac{2\gamma V}{r} \tag{7}$$

Absorption performance as a Function of the Nanoparticle Concentration

The absorption experiments were performed by changing the fraction of nanoparticles in the nanofluid from 0.01 wt% to 0.04 wt%, as shown in Fig. 12. From the results, the absorption performance increases with increasing nanoparticle content. This suggests that a large amount of nanoparticles induces positive effects on the gas absorption mechanism because a large amount of nanoparticles presents more energy to the solution and effectively reduce the gas bubble size.

Size Effects of Nanoparticles on Absorption Performance

Gas absorption experiments were performed in the three different nanofluids containing three different sized nanoparticles of 30 nm, 70 nm, 120 nm, respectively, and the same nanoparticle fraction of 0.021 wt%.

From the results of Fig. 13, all the three graphs almost coincided with each other and do not show large changes depending on the particle size.

One possible explanation is that the same content of nanofluid presents the same amount of additional energy to the solution, because the number of nanoparticle is increased by decreasing the particle size and decreased by increasing particle size. The gas bubbles in the same contents of nanofluid are cracked to the same size even at the different sizes of the nanoparticles and result in the same absorption performance.

CONCLUSION

In this study, three kinds of nanofluids containing 30 nm, 70 nm, 120 nm particles were synthesized. The zeta potential values of all nanofluids were approximately −45 mV, and were judged to be stable. The average CO_2 absorption rate during the first 1 minute, and the total absorption in the 0.021 wt% nanofluid increased 76% and 24% respectively, compared to water. The capacity coefficient in the nanofluid and water were found to be 0.045 s^{-1} and 0.0105 s^{-1}. In the piperazine/K_2CO_3 absorbent, the average CO_2 absorption rate during the first 1 minute and total absorption were increased 11% and 12% by the addition of 0.021 wt% nanoparticles. In this research, studies on the synthesis and characterization of the nanofluids will form the basis for an in-depth nanoparticles and fluid technology for many applications. The CO_2 absorption processes in the nanofluid with a piperazine/K_2CO_3 solution are directly applicable to the industrial plants for reduction of CO_2.

NOMENCLATURE

V_A: Van der Walls attractive energy[J/m^2]
A: Hamaker Constant[J]
d: Distance between two particles[m]
V_R: Double layer repulsive energy[J/m^2]
V_0: Surface change density[J/m^2]
k: Inverse debye length [m]
V_T: Total energy [J/m^2]
W_A: Absorption rate [L/min]
V: Inner volume of a bubble type absorber [L]
k_La: Capacity coefficient[/s]
$C_{A,S}$: Concentration at the film surface [mol/L]
C_A: Concentration at some point in the fluid phase [mol/L]
R_A: Reaction rate[/s]

R: Gas constant[J/ mol.K]
T: Tempaarature [K]
P^r: Vapor pressure [pa]
P^{∞}: isotropic pressure [pa]
γ: surface tension [N/m]
{{\overline{V}_{L}}}: Molar volume of liquid [L/ mol]
r: b*ubbleradius* [*m*]

ACKNOWLEDGEMENT

This study was supported by research grants from the Korea Science and Engineering Foundation(KOSEF, ERC) through the Applied Rheology Center(ARC) at Korea University, Seoul, Korea.

REFERENCES

1. Xun, F.; Wei, Y.; Yusheng, L.; Debao, W.; Huaqiang, S.; Fengyuan, Y.(2005) Preparation of Concentrated Stable Fluids Containing Silver Nanoparticles in Nonpolar Organic Solvent. *J. Disper. Sci. Technol.*, *26*: 575–580.
2. Christopher, L.; Christopher, B. (2006) Copper Nanoparticle Synthesis in Compressed Liquid and Supercritical Fluid Reverse Micelle Systems. *Ind. Eng. Chem. Res. 43*: 6070–6081.
3. Lai, J.; Shafi, V.; Ulman, A.; Loos, K.; Lee, Y.; Vogt, T.; Lee, W.; Ong, N. (2005) Controlling the Size of Magnetic Nanoparticles Using Pluronic Block Copolymer Surfactants. *J. Phys. Chem. B.*, *109*: 15–18.
4. Choi, S.U.S. (1995) Enhancing thermal conductivity of fluids with nanoparticles. *Development and Application of Non-Newtonian Flows*, *231*: 99–105.
5. Zhang, X.; Gu, H.; Fujii, M. (2007) Effective thermal conductivity and thermal diffusivity of nanofluids containing spherical and cylindrical nanoparticles. *Exp. Therm. Fluid Sci.*, *31*: 593–599.
6. Heris, S.Z.; Esfahany, M.N.; Etemad, S.Z. (2007) Experimental investigation of convective heat transfer of Al_2O_3/water nanofluid in circular tube. *Int. J. Heat Fluid Fl.*, *28*: 203–210.
7. Keblinski, P.; Phillpot, S.R.; Choi, S.U.S. (2002) Eastman JA. Mechanisms of heat flow in suspensions of nano-sized particles. *Int. J. Heat Mass Tran.*, *45*: 855–863.
8. Krishnamurthy, S.; Bhattacharya, P.; Phelan, P.E. (2006) Enhanced Mass Transport in Nanofluids. *Nano Lett.*, *6*: 419–423.
9. Ha, J.J. (2002) Characteristics of Heat and Mass transfer properties by using silica nanoparticles in ammonia-water system. MA thesis, Korea University, Korea.

10. Kim, J.K.; Jung, J.Y.; Kim, J.H.; Kim, M.G.; Kashiwagi, T.; Kang, Y.T. (2006) The effect of chemical surfactants on the absorption performance during NH_3/H_2O bubble absorption process. *Int. J. Refrig.*, *29*: 170–177.
11. Astarita, G. (1961) Carbon dioxide absorption in aqueous monoethanolamine solutions. *Chem. Eng. Sci.*, *16*: 202–207.
12. Chakraborty, A.K.; Astarita, G.; Bischoff, K.B. (1986) CO_2 absorption in aqueous solutions of hindered amines. *Chem. Eng. Sci.*, *41*: 997–1003.
13. Rao, D.P. (1990) Design of a packed column for absorption of carbon dioxide in DEA promoted hot K_2CO_3 solution. *Gas Sep. Purif.*, *4*: 58–61.
14. Cullinane, J.T.; Rochelle GT. (2004) Carbon dioxide absorption with aqueous potassium carbonate promoted by piperazine. *Chem. Eng. Sci.*, *59*: 3619–3630.
15. Derks, P.W.J.; Kleingeld, T.; Aken, C.V.; Hogendoorn, J.A.; Versteeg, G.F. (2006) Kinetics of absorption of carbon dioxide in aqueous piperazine solutions. *Chem. Eng. Sci.*, *61*, 6837–6854.
16. Dagaonkar, M.V.; Heeres, H.J.; Beenackers, Pangarkar, V.G. (2003) The application of fine TiO_2 particles for enhanced gas absorption. *Chem. Eng. J.*, *92*: 151–159.
17. Kim, S.H.; Kim, W.G.; Kang, H.U. Gas absorption device comprising nanoparticles dispersed in fluid. Korea patent. 10–0691859–0000, February 28, 2007.
18. Song,K.C.; Park, J.K.; Kang, H.U.; Kim, S.H. (2003) Synthesis of Hydrophilic Coating Solution for Polymer Substrate Using Glycidoxypropyltrimethoxysilane, *J. Sol-Gel Sci. Technol.*, *27*: 53–59.
19. Evans, D.F.; Håkan Wennerström. (1994) The Colloidal Domain: Where Physics, Chemistry, Biology, and Technology Meet.; Wiley-VCH., 333–338.
20. Rao, K.S.; Khalil, E.H.; Kodaki, T.; Matsushige, K.; Makino, K. (2005) A novel method for synthesis of silica nanoparticles. *J. Colloid. Interf. Sci.*, *289*: 125–131.
21. Welty, J.R.; Wicks, C.WicksE.; Wilson, R.E.; Rorrer G.L. (2000) *Fundamentals of Momentum, Heat, and Mass Transfer* 4th Ed.; John Wiley & Sons: New York, 622.
22. Adamson, A.W.; Gast, A.P.(1997) *Physical Chemistry of Surfaces* 6th Ed.; John Wiley & Sons: New York, 57.